Preclinical development and optimization of novel PD-L1 tracers and first-in-human study of [^{68}Ga]Ga-NOTA-RW102 in cancer patients

You Zhang[1,#], Min Cao[2,#], Yanfei Wu[3,#], Sara Malih[4,5], Dong Xu[6], Erpeng Yang[1], Muhsin H. Younis[4], Wilson Lin[4], Haitao Zhao[1], Cheng Wang[1], Qiufang Liu[7], Jonathan W. Engle[4], Mohammad J. Rasaee[5], Yihui Guan[3], Gang Huang[1], Jianjun Liu[1,*], Weibo Cai[4,*], Fang Xie[3,*], Weijun Wei[1,*]

[1] Department of Nuclear Medicine, Institute of Clinical Nuclear Medicine, Renji Hospital, School of Medicine, Shanghai Jiao Tong University, Shanghai 200127, China.

[2] Department of Thoracic Surgery, Renji Hospital, School of Medicine, Shanghai Jiao Tong University Shanghai 200217, China.

[3] Department of Nuclear Medicine & PET Center, Huashan Hospital, Fudan University, Shanghai.

[4] Departments of Radiology and Medical Physics, University of Wisconsin−Madison, Madison, WI, USA.

[5] Department of Medical Biotechnology, Faculty of Medical Sciences, Tarbiat Modares University, Tehran, Iran.

[6] Department of Thoracic Surgery, Huashan Hospital, Fudan University, Shanghai 200040, China.

[7] Department of Nuclear Medicine, Fudan University Shanghai Cancer Center, Fudan University, Shanghai 200030, China.

[#] These authors contributed equally to the work.

* **Corresponding Authors:**

Prof. Weijun Wei

Department of Nuclear Medicine, Renji Hospital, School of Medicine, Shanghai Jiao Tong University, Shanghai 200127, China; e-mail: wwei@shsmu.edu.cn.

Prof. Fang Xie

PET Center, Huashan Hospital, Fudan University, Shanghai 200040, China; e-mail: fangxie@fudan.edu.cn.

Prof. Weibo Cai

Departments of Radiology and Medical Physics, University of Wisconsin−Madison, Madison, WI, USA. E-mail: wcai@uwhealth.org.

Prof. Jianjun Liu

Department of Nuclear Medicine, Institute of Clinical Nuclear Medicine, Renji Hospital, School of Medicine, Shanghai Jiao Tong University, Shanghai 200127, China. E-mail: nuclearj@163.com.

Supplemental Information

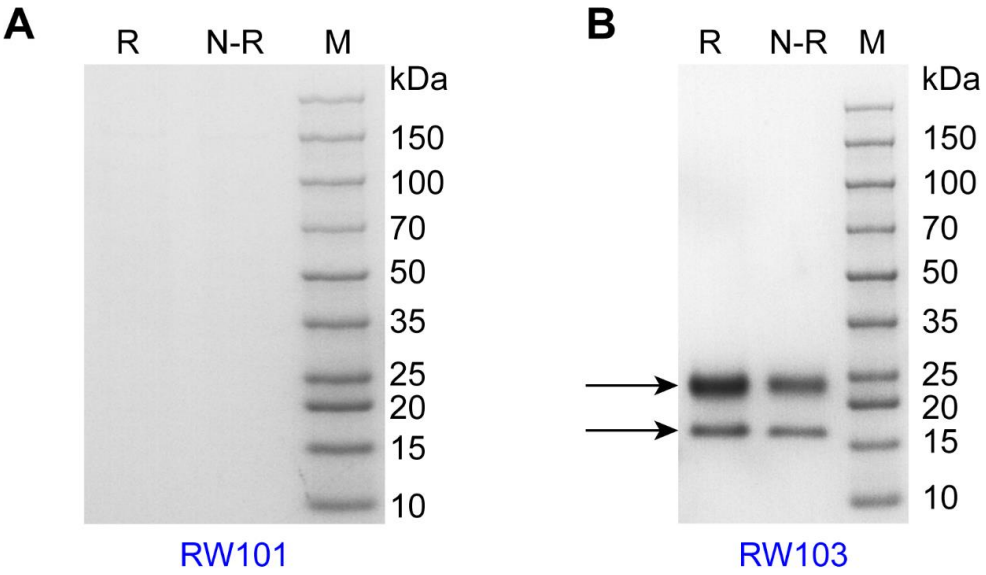

Figure S1: SDS-PAGE analysis of RW101 (A) and RW103 (B) cloned in pET-30a(+) and expressed in BL21(DE3) strain. R: reducing; N-R: non-reducing; M: marker.

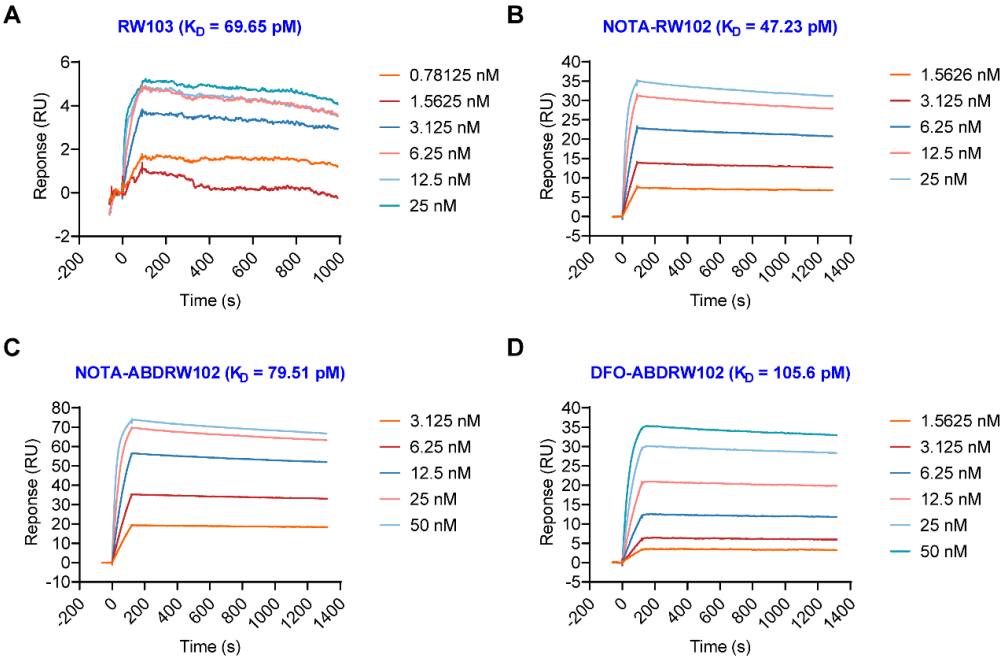

Figure S2: The surface plasmon resonance (SPR) studies showed the association and dissociation kinetics of RW103 (A), NOTA-RW102 (B), NOTA-ABDRW102 (C), and DFO-ABDRW102 (D) interacting with recombinant human PD-L1 protein.

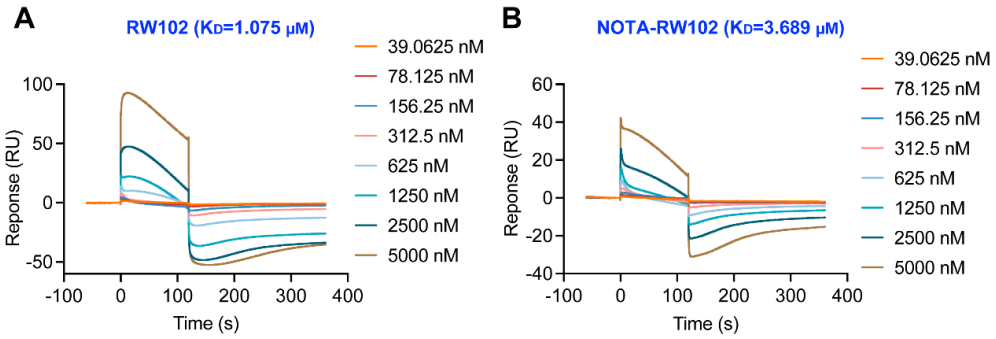

Figure S3: The surface plasmon resonance (SPR) studies showed the association and dissociation kinetics of RW102 (A) and NOTA-RW102 (B) interacting with mouse PD-L1 protein.

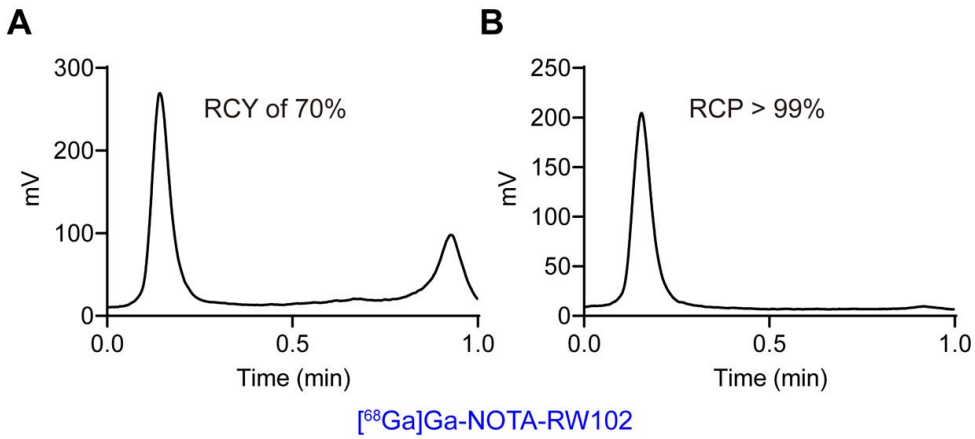

Figure S4: The radiochemical yield (A) and radiochemical purity (B) of [^{68}Ga]Ga-NOTA-RW102 assessed by instant thin-layer chromatography.

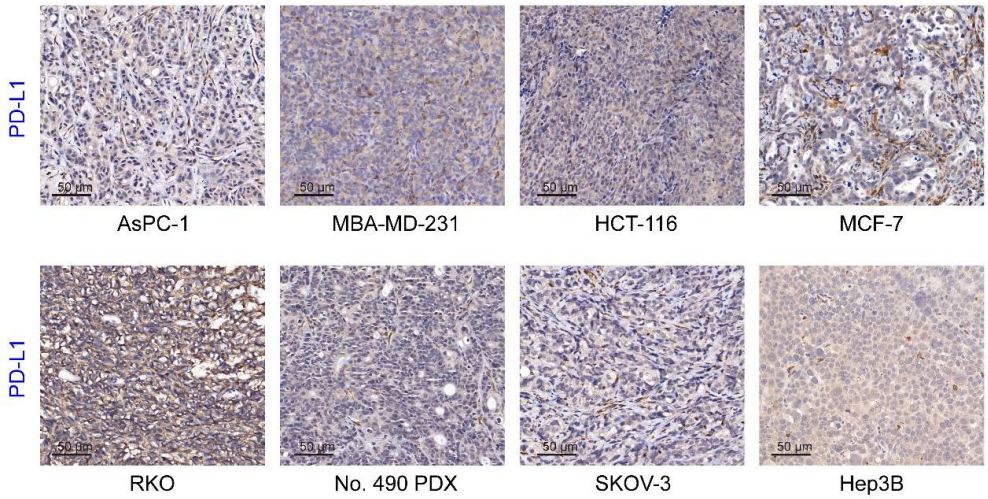

Figure S5: Immunohistochemical staining of PD-L1 expression in different types of tumors.

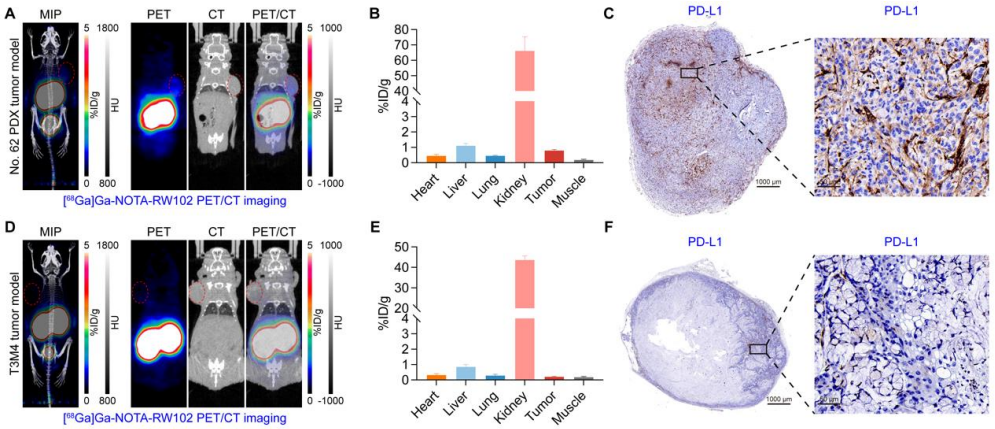

Figure S6: [^{68}Ga]Ga-NOTA-RW102 immunoPET imaging in No. 62 renal cancer PDX models (A, B) and T3M4 tumor models (D, E) 0.5 h post-injection of the tracer. Red dotted circles showed the tumors. The PD-L1 antigen immunohistochemical staining of No. 62 renal cancer PDX tumor (C) and T3M4 tumors (F).

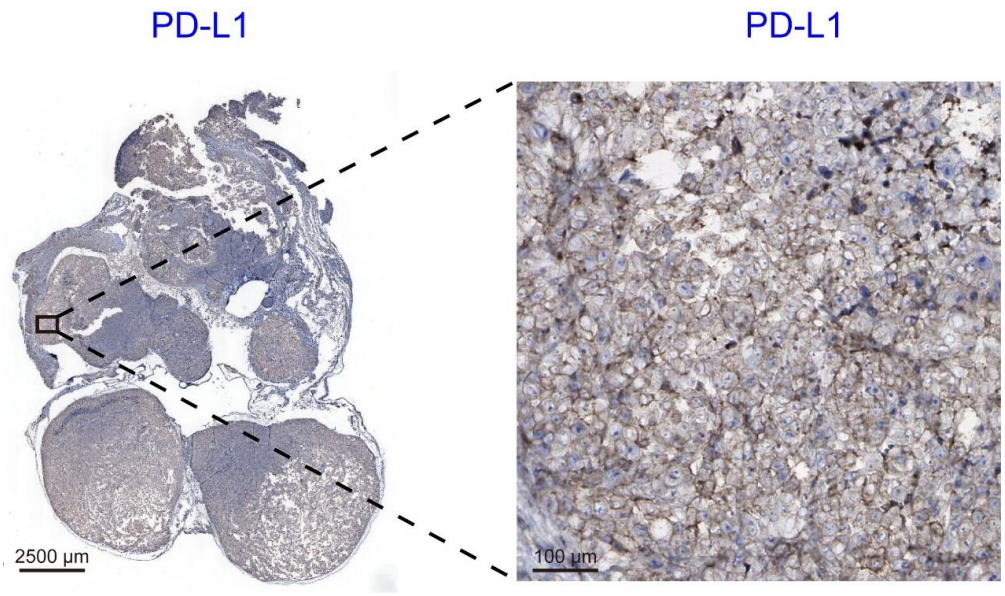

Figure S7: The PD-L1 antigen immunohistochemical staining of A375-PD-L1 tumors.

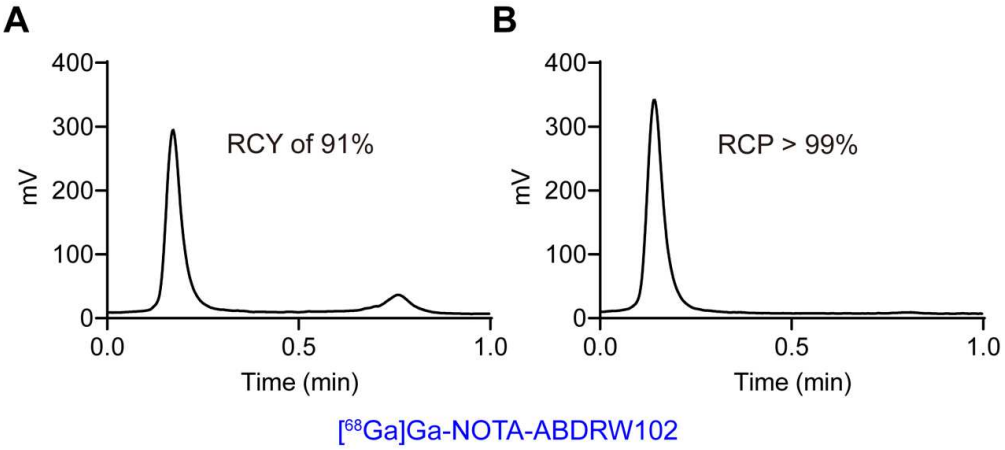

Figure S8: The radiochemical yield (A) and radiochemical purity (B) of [^{68}Ga]Ga-NOTA-ABDRW102 assessed by instant thin-layer chromatography.

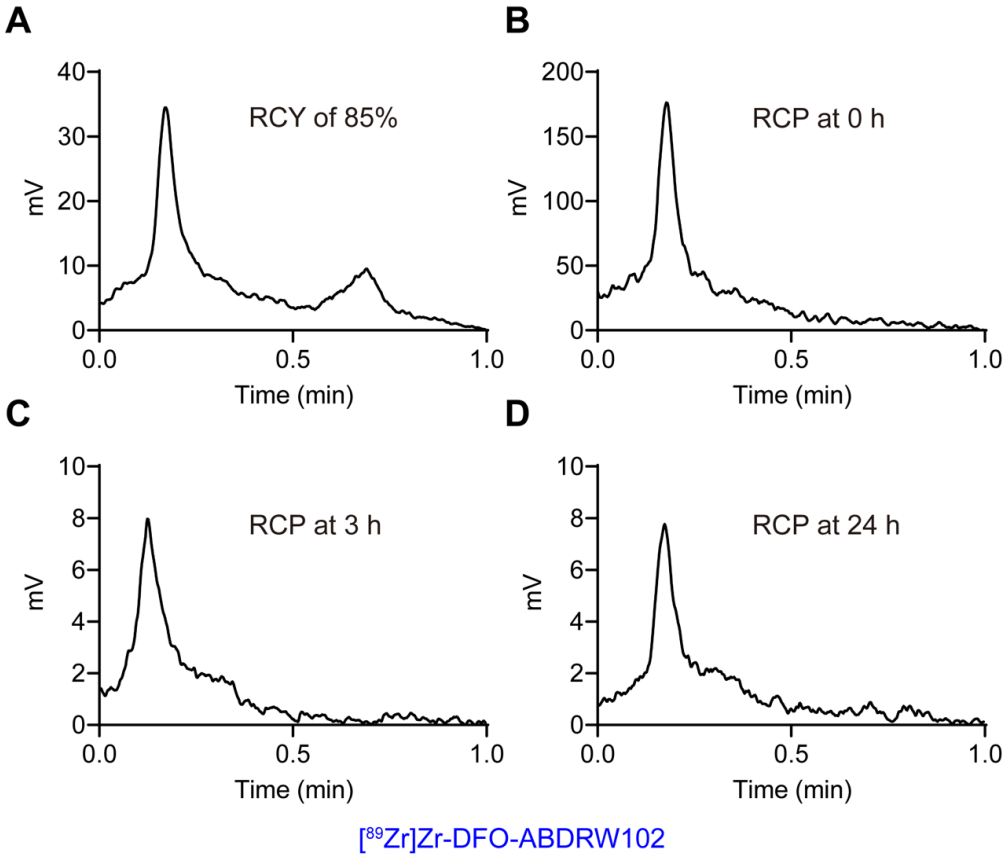

Figure S9: The radiochemical yield (A), instant radiochemical purity (B), and stability in PBS solution at 3 h (C) and 24 h (D) of [^{89}Zr]Zr-DFO-ABDRW102 assessed by instant thin-layer chromatography.

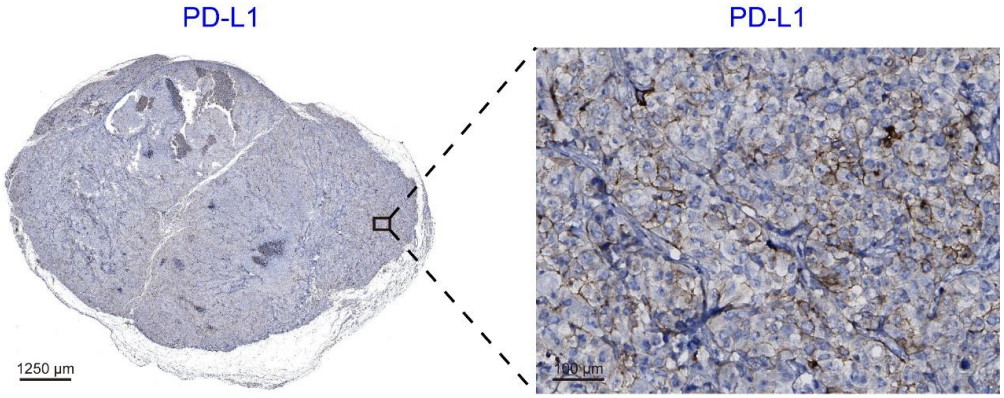

Figure S10: Immunohistochemical staining of PD-L1 expression in LM3-PD-L1 tumors.

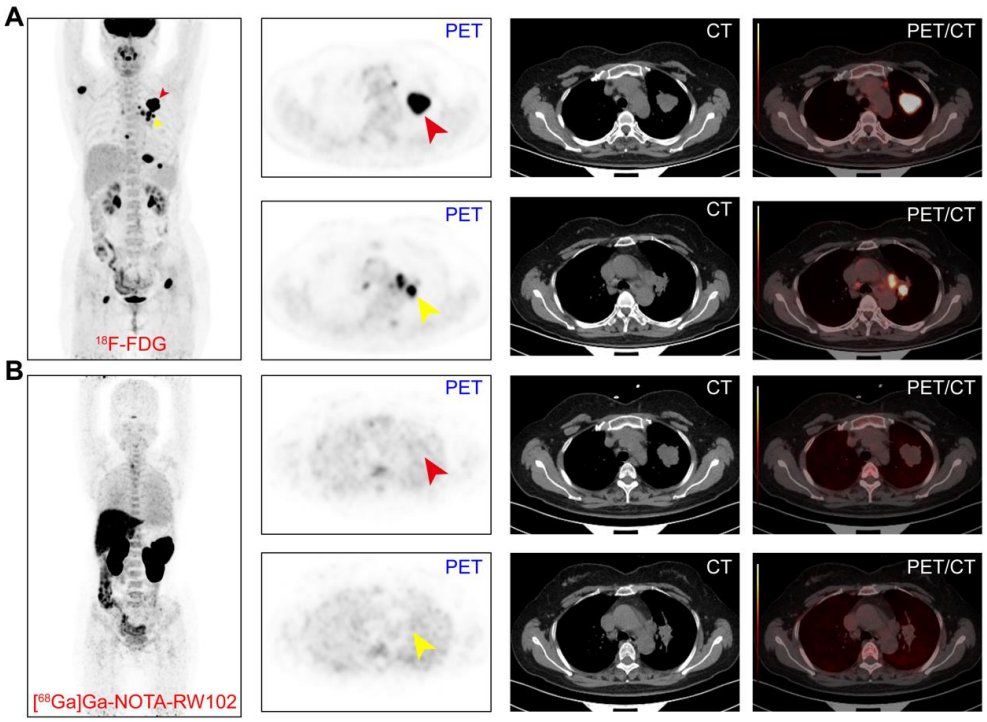

Figure S11. ^{18}F-FDG and [^{68}Ga]Ga-NOTA-RW102 immunoPET imaging of a patient with 2% PD-L1 expression. (A) ^{18}F-FDG images of the patient showing the primary tumor and multiple metastases across the body (The red arrow shows the left upper lobe lesion, and the yellow arrow shows the left hilar lymph node metastases; from left to right: MIP image, PET images, CT images, and PET/CT fused images). (B) [^{68}Ga]Ga-NOTA-RW102 PET/CT images of the patient (The red arrow shows the left upper lobe lesion and the yellow arrow shows the left hilar lymph node metastasis; from left to right, MIP image, PET images, CT images, and PET/CT fused images).

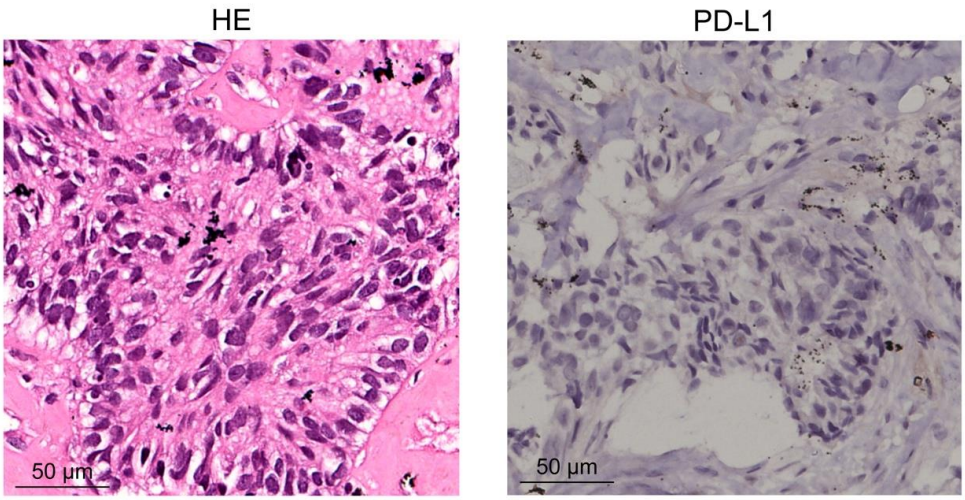

Figure S12: HE staining and PD-L1 antigen immunohistochemical staining of the patient's left upper lobe lesion. The results showed a low PD-L1 expression (2%).

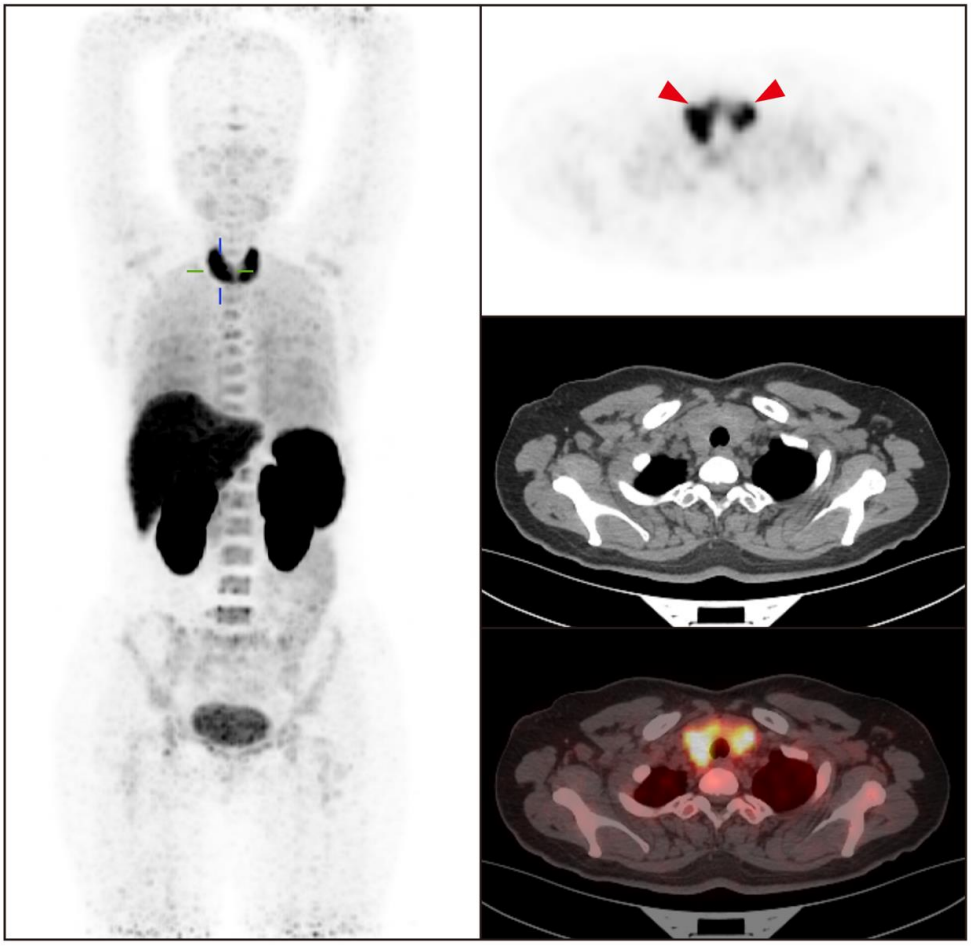

Figure S13: Images of an adult patient with left lower lung adenocarcinoma and thyroiditis (left image: MIP image; Right images from top to bottom: PET image, CT image, and PET/CT fused image).

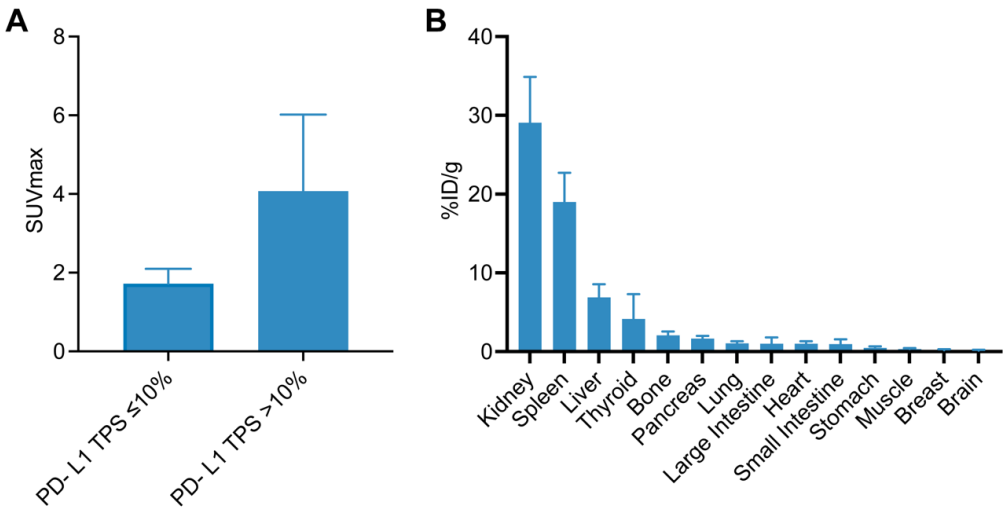

Figure S14: (A) The different SUVmax corresponding to different PD-L1 expressions. (B) The [^{68}Ga]Ga-NOTA-RW102 uptake and distribution profiles in normal tissues and organs.

Table S1: Patient characteristics.

Patient	Pathological typing	PD-L1	SUVmax of the primary tumor	Injection dose (MBq)
1	Adenocarcinoma	40%	1.17	111
2	Adenocarcinoma	20%	2.4	101
3	Squamous carcinoma	1%	1.17	111
4	Adenocarcinoma	<1%	2.03	92.5
5	Adenocarcinoma	2%	1.86	74
6	Squamous carcinoma	70%	5.45	74
7	Adenocarcinoma	80%	NA	111
8	Adenocarcinoma	10%	NA	167
9	Adenocarcinoma	10%	1.82	118
10	Adenocarcinoma	NA	NA	62.9

NA: Not acquired.